INVESTIGATION OF SPACE VEHICLE MOTION IN THE ATMOSPHERE

D.Ye.Okhotsimskiy and N.I.Zolotukhina

N65-23673

FACILITY FORM 602

(ACCESSION NUMBER)   (THRU)

(PAGES)   (CODE)
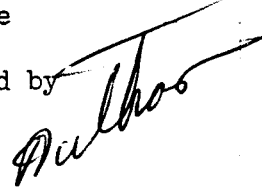
30

(NASA CR OR TMX OR AD NUMBER)   (CATEGORY)

INVESTIGATION OF SPACE VEHICLE MOTION IN THE ATMOSPHERE   */1

D.Ye.Okhotsimskiy and N.I.Zolotukhina

The motion of a spacecraft in the atmosphere, after reentry through the reentry "corridor" with special emphasis on the g-loading, is described. Descent trajectories with local parabolic velocity at an altitude of 100 km, using the height of perigee as the basic parameter, are calculated for fixed and variable L/D. Descent path length, g-loading, and altitude are plotted against time and limit values for g-loading are given. To prevent narrowing of the reentry corridor by reduction in g-value, control of lift by two change-overs from maximum positive to maximum negative value is recommended for path lengths of 10,000 km and by up to four change-overs for lengths of 5000 km.

The motion of a space vehicle in the atmosphere is investigated in this paper, and an analysis is offered of the possibilities of using low lift to reduce the requirements for reentry accuracy and to decrease g-loading during reentry into the atmosphere at second cosmic (escape) velocity.

An examination is made of descent trajectories which have a local parabolic velocity at an altitude of y_0 = 100 km. The reentry angle θ (angle between the transversal and velocity at altitude y_0) is uniquely determined by the height of the osculating perigee h, i.e., the height of orbital perigee in unperturbed motion and in the absence of atmospheric resistance.

---

* Numbers in the margin indicate pagination in the original foreign text.

The perigee height uniquely characterizes reentry conditions for a trajectory with a given energy. The selection of perigee height as a basic parameter makes it possible to relate the outside portion of the trajectory to the descent portion in the atmosphere, in the most natural manner. It is found convenient to compute the length of the descent portion and the time along the trajectory from the instant which would correspond to passage of the perigee in unperturbed motion.

The spread of perigee heights for which a descent with a given length can be realized is called the "corridor width with respect to perigee height". The wider the reentry corridor the less accuracy is required during approach of the space vehicle to the Earth, prior to descent.

Control of lift of the space vehicle permits a reduction in g-loading. If we establish the maximum allowable g-level, then control of lift can be utilized in order to provide as large a reentry corridor as possible.

Let us assume that the control of lift bears the character of a change- /2 over from the maximum possible positive value to the maximum possible negative value, and vice versa. With this relay character of lift variation, the problem is then reduced to an optimum selection of the number of and instants for change-over.

An examination is made first of a descent with fixed L/D (without change-over). Following this, we examine descents with one, two, and more change-overs. An analysis is given of the character of g-variation during vehicle motion and the position of the maximum. G-load and perigee height spreads are examined. In the calculations performed here, standard atmosphere (Bibl.1) was approximated and used.

1. Descent with Fixed L/D

The investigation of a descent with a fixed L/D value was carried out with the aim of revealing the spread of perigee heights for which such a descent is possible, and also for the purpose of determining the g-loads prevailing in this case. Here and in the following discussion we shall deal with values of total g, determined by the formula:

$$n = cv^2 \, \Delta \sqrt{1 + \varkappa^2}$$

where v is the velocity modulus, $\varkappa = \dfrac{C_L}{C_D}$ is the L/D ratio, C_D and C_L are the aerodynamic coefficients of drag and lift, $c = \dfrac{1}{2} \dfrac{g_0 \rho_0 S}{G} C_D$ is the ballistic coefficient, g_0 and ρ_0 are the acceleration of gravity and the air density at the Earth's surface, S is the characteristic surface, G is the weight of the vehicle, and $\Delta = \dfrac{\rho}{\rho_0}$ is the density ratio. In our calculations, the ballistic coefficient is taken as c = 1 l/km.

Let the vehicle have an L/D of $\overline{\varkappa}$. This means that the L/D can take on any value within the range of regulation, i.e., in the range $-\overline{\varkappa} \leq \varkappa \leq \overline{\varkappa}$. A /3 negative L/D is understood to be one that corresponds to a negative value of lift.

Let h_1 be the height of perigee of a trajectory having a length L during the descent with fixed positive L/D; h_3 is the height of perigee of a trajectory which has the same length during a descent with fixed negative L/D. The spread of perigee heights $h_1 \leq h \leq h_3$ is the reentry corridor with respect to the height of the perigee for a given length L and a L/D of $\overline{\varkappa}$. This means that for any height h from the reentry corridor, it is possible to select an L/D in the range of control such that, during descent with fixed L/D, the descent trajectory will have the length L. The determination performed for the reentry

3

corridor proceeds only from the condition of attaining the given length. If we accept additional limitations, for example, with respect to considerations of heating conditions or with respect to g, this may lead to a narrowing of the corridor.

G-forces along the trajectory vary non-monotonically, forming a series of maximums whose magnitude and distribution depend on the magnitude of the prevailing L/D and the height of the perigee. Main emphasis was placed on the magnitude of the greatest maximum.

Figures 1 and 2 present the results of calculations performed to demonstrate the possibilities of descent with fixed L/D. The abscissa gives the perigee height; to the left of the ordinate axis we entered the distance L = = φR (φ being the terminal angular distance reckoned from the perigee, and R the Earth's radius); to the right of the ordinate axis are the magnitudes of peak-g denoted by n. Figure 2 shows, in a rougher scale, the region of perigee heights which corresponds to L/D values $\varkappa \leq 0.3$.

The solid lines on the graphs represent the correlation of length to   /4 perigee height for a given L/D. As can be seen from the graphs for descent trajectories with constant lift/drag ratio $\varkappa$, there is a limit perigee height $\overline{h}(\varkappa)$ depending upon the L/D. The trajectories which have perigee heights of $h > \overline{h}(\varkappa)$ do not descend to the Earth's surface on the first pass. For trajectories with perigee heights of $h < \overline{h}(\varkappa)$ there is a single-valued relationship between perigee height and length L. As the perigee height drops, the length decreases.

The broken lines in Figs.1 and 2 represent a family of curves which show the relationship of peak-g to perigee height for trajectories of a given length. As can be seen from the graphs, along the curves in this family, in the region

4

of perigee heights of the order of 50 - 60 km, the g-forces show a minimum of approximately n = 5. These minimum g-values occur at an L/D of $\varkappa$ = 0.1 - 0.15. In the indicated region, the first and second g-maxima are close to each other. For heights of h < 50 km, the first g-maximum is the greatest and the determining one; for heights of h > 60 km, the second maximum is greatest.

Figure 2 also presents a family of lines matching the g-values for a fixed L/D. These lines consist of two segments separated by a small cross. The first segment (thin lines) corresponds to the peak g-forces on the descending trajectories. The second segment (dot-dash lines) corresponds to g-forces generated during passage through the atmosphere on trajectories which do not descend to the Earth on the first pass. As can be seen from the graph, the g-forces on the second segment are comparatively small. These g-forces can be attained also on descending trajectories if a change-over of L/D is employed /5 in the process of descent. This will be dealt with in more detail below. We should like to point out, as can be seen from the graph in Fig.2, that the relationship of g-force at a given L/D to perigee height for $\varkappa \gtrsim$ 0.1 is close to linear.

The peak-g is practically independent of the ballistic coefficient whose magnitude has an effect only on the altitude of passage through maximum g. If we assume an exponential law for the variation in density with altitude then the shift of g-maxima with respect to altitude, for a variation in the ballistic coefficient of Δc, can be estimated in the form

$$\Delta y = H\ell n \frac{c_1}{c_2}$$

where H is the altitude of the homogeneous atmosphere, $c_1 = c_0 + \Delta c$. Thus, for example, with a two-fold increase in the ballistic coefficient $\left(\dfrac{c_1}{c_0} = 2\right)$,

assuming the altitude of the homogeneous atmosphere to be H = 8 km which corresponds to a deceleration altitude of 50 - 60 km, we obtain a shift with respect to the altitude Δy = 6 km in the region of great altitudes. The correctness of such a recalculation was substantiated in the performed computations. A variation in the ballistic coefficient leads to a parallel shift of the graphs with respect to perigee height. In this case, the width of the reentry corridor is not altered.

It is clear from the graphs presented that the introduction, into this investigation, of trajectories with large L/D values will ensure obtaining an adequately wide reentry corridor. However, the g-values in the entire corridor may be very large. Introducing a limitation on the magnitude of g will lead to a sharp narrowing of the corridor.

The relationship of reentry corridor width to the allowable magnitude of g during descent with a fixed L/D is shown in Fig.3. The abscissa gives the <u>/6</u> allowable g-value and the ordinate, the width of the reentry corridor. The solid lines show the ratio of reentry corridor width to allowable g-value for a given length of the descent path; the broken lines correspond to fixed L/D values.

It can be seen from the graph how a reduction of the allowable g-value diminishes the width of the reentry corridor. For example, if the allowable g-value is taken as n = 40, then for a trajectory of L = 5000 km, the width of the reentry corridor will be Δh = 360 km. To achieve the indicated reentry corridor, the vehicle must have an L/D of $\bar{\varkappa} \geq 1$. If we limit the allowable g-value to n = 10, then, for the same length, the width of the reentry corridor will be $\Delta h \approx 50$ km, in which case it is necessary for the vehicle to have an L/D of $\bar{\varkappa} \geq 0.3$. The graph in Fig.3 shows that a reduction in the allowable g-value

6

causes a decrease in the L/D magnitude needed to achieve the corridor which satisfies the accepted magnitude for the allowable g.

2. Descent with Change-Over

As pointed out above, a relay system of L/D change-over was investigated for the purpose of controlling the L/D. We reviewed descent patterns with a varied number of L/D change-overs from maximum positive L/D to negative and vice versa. In all of the studied patterns it was assumed that the change of L/D occurs instantaneously; transient processes were not investigated.

Two patterns were examined with a single L/D change: one pattern with an L/D change from negative to positive and one with an L/D change from positive to negative. /7

In the first pattern, it was assumed that the reentry of the vehicle into the atmosphere in the first moments is accompanied by a lift which is directed downward $(\varkappa = -\bar{\varkappa})$, so that the aerodynamic force pushes the vehicle toward the Earth. Then, at the instant t_1, the direction of lift changes and the further descent proceeds with an upward-directed lift $(\varkappa = \bar{\varkappa})$. Attainment of the given length of the descent portion is ensured by selecting the instant of change-over t_1.

In the second pattern which incorporates a single variation of L/D, it was assumed that initial reentry into the atmosphere takes place at a positive L/D. Then, at some instant of time the L/D instantaneously becomes negative and remains negative until the descent is terminated. In the case of such a descent pattern, extremely large g-forces develop after the second dip into the atmosphere; hence, this pattern is not rational. However, the pattern is of interest from the point of view of determining the instant of time for change-over $\bar{t}_1$ (L),

7

which will yield the desired length L. As it turned out, the instant $\bar{t}_1$ apparently is very close to the optimum instant for the first change-over in the case of a pattern with more than one change-over.

The instant $\bar{t}_1$ may be called the "boundary of controllability" of a trajectory of length L, since with no manner of L/D change-over, when $t > \bar{t}_1(L)$, can the length L be obtained (the length is larger than the given length or the trajectories do not descend to the surface of the Earth on the first pass).

Let us examine a pattern with a two-time variation of the direction of $\underline{/8}$ lift. Let the first portion of the descent from the altitude y_0 to the instant of the initial change-over proceed at positive lift ($\varkappa = \bar{\varkappa}$). At the instant t_1 the direction of lift reverses and a certain portion of the trajectory is then traversed at a negative L/D ($\varkappa = -\bar{\varkappa}$). Then, at the instant t_2 the L/D value again becomes positive and remains positive to the termination of the descent.

The physical sense of the investigated variation in lift during the descent consists in a tendency toward reduction of the curvature of the trajectory and a prolonging of the duration of the deceleration portion. Protracted deceleration in the upper layers of the atmosphere leads to a situation wherein a considerable part of the velocity is lost in the upper layers of the atmosphere, the variation in g with respect to time is considerably stretched out, and the peak-g is lowered.

A pattern with two change-overs contains the two parameters t_1 and t_2 which are related by the condition for achieving the given length. For given values of lift/drag ratio, length, and perigee height, we find a single-parameter family of trajectories. The magnitude of peak-g along the trajectories of this family varies. It is necessary to find that trajectory for which the peak-g is smallest.

8

Figures 4 and 5 for a pattern with two change-overs, show the relationship of g-loading to time for trajectories with a length of L = 5000 km and for an L/D of $\bar{\varkappa}$ = 0.5, for the case of the two perigee heights h = 44 km and h = 54 km, respectively. The set of trajectories has a free parameter. To represent this parameter, we will select the instant t_1 of the initial change-over.

The family of trajectories is bounded by two limit trajectories. The /9 first limit trajectory corresponds to a descent with one change-over from $-\bar{\varkappa}$ to $+\bar{\varkappa}$. This can be viewed as the limit case for $t_1 = t_0$ and the pattern with two change-overs degenerates into a pattern with one L/D change-over. This is represented by curve I in Figs.4 and 5. The other limit trajectory is the trajectory with one change-over from $+\bar{\varkappa}$ to $-\bar{\varkappa}$. This can be considered as the limit case for the instant of the second change-over $t_2 = t_{ter.}$ where $t_{ter.}$ is the terminal instant of motion. In Figs.4 and 5 this boundary of the family of trajectories is represented respectively by curves VII and VIII. The instants of the initial change-over t_1 for the trajectories of this family are included in the interval $t_0 \leq t_1 \leq \bar{t_1}$.

In Figs.4 and 5, the heavy broken line connects the maxima for g-loading on trajectories with different values of t_1. These graphs indicate that both limit trajectories are highly unsuitable from the point of view of g-loading.

Let us examine the evolution of the relationship of g-loading to time for the case of variation of the parameter t_1 in the allowable region. For values of t_1 close to t_0, an increase in t_1 will lead to a reduction in the maxima of g-loading. After t_1 has passed through the value t_{1m}, which corresponds to the moment of the first g-loading maximum, still another maximum occurs close to the first maximum (see curves II and III in Figs.4 and 5). With a further increase in t_1, the first isolated maximum does not change, while the magnitude

of the second maximum is reduced. In addition, there is a simultaneous lower-
ing of all succeeding maxima. However, beginning from some instant immediately
at the boundary of $\bar{t}_1$, the g-forces begin to increase sharply.

The first of the graphs presented (Fig.4), which corresponds to the
lesser perigee height, shows that in the case of a minimization of g-loading
the magnitude of the first maximum is larger than all of the succeeding maxima.
In this case, the instant t_1 can be selected in such a manner that the succeed-
ing maxima will be as small as possible.

The second graph (Fig.5), which corresponds to the larger perigee height,
shows that for all trajectories close to the optimum the second g-loading maxi-
mum is largest.

Let h_2 be the height of perigee of a trajectory with two change-overs, for
which equality is achieved between the first and one of the succeeding maxima
of g-loading. The reentry corridor can then be divided into two portions, in
which the character of g-minimization will differ.

If the perigee of the trajectory h is located in the first portion of the
reentry corridor ($h_1 < h < h_2$) (see, for example, Fig.4) then, in order that
g-loading be minimal, the first change-over must occur after passage of the
first maximum, obviously, by selecting the instant for change-over from the
interval $t_{1m} < t_1 < \bar{t}_1$. The magnitude of the first maximum will be the deter-
mining one. The magnitude of the first maximum cannot be reduced by manipula-
tion of the change-over pattern.

The trajectories in Fig.5 correspond to the height of perigee from the
second portion of the reentry corridor $h_2 < h < h_3$. As a result of g-minimiza-
tion, the second maximum of g-loading is largest. By manipulating the pattern
and increasing the number of change-overs it is possible to reduce this second

10

maximum. As an example of this reduction, we show a trajectory with four change-overs in Fig.6. As initial condition for this trajectory we selected an optimum trajectory with a height of perigee h = 54 km, obtained as a result of g-minimization with a pattern containing two change-overs. The g-loading on <u>/11</u> this trajectory is shown in Fig.5 by curve IV. A comparison of the graphs indicates that an increase in the number of change-overs up to four resulted in an essential reduction of g-loading.

In Figs.7 and 8 the altitude variation is plotted as a function of time for the trajectories whose g-loading is represented in Figs.4 and 5. It can be seen from the graphs presented that the first three trajectories ricochet considerably, rising to an altitude of y = 150 km or more. All the succeeding trajectories, including trajectory IV, which represents optimum g-loading, have the character of a creeper. The minimum altitude during the first dip increases with the growth in t_1. The first trajectory, which corresponds to the limit trajectory I in Fig.4, dips into the atmosphere to an altitude of y = 50 km. For the optimum trajectories, corresponding to curves IV, the altitude on the first dip increases to 65 - 68 km.

The graphs in Figs.4 - 8 and their descriptions are presented as examples which characterize the variation in altitude and g-loading for descent trajectories with a length of L = 5000 km for an L/D of $\bar{\varkappa}$ = 0.5. For trajectories which have a greater length (for example, L = 10,000 km) with perigee heights lying in the second region of the reentry corridor, the largest maximum is not the second but rather the last maximum, which occurs upon final penetration into the atmosphere.

Similarly, as was done for an L/D of $\bar{\varkappa}$ = 0.5, we worked out the process of g-minimization for other L/D values as well. At $\bar{\varkappa}$ ≤ 0.3, the difference

from trajectories with $\bar{\varkappa} \leq 0.5$ consists in the fact that, in the second region of the reentry corridor, the largest maximum is the last maximum, while the second maximum can always be reduced and made lower than the first maximum by proper selection of the instant for change-over.

Calculations were performed for varying values of length and L/D. A resumé of the results is set forth in the Section which follows.

3. Limit Values for G-Loading

Summary graphs, characterizing the limit values of g-loading during a descent with L/D change-over, are presented in Fig.9. The abscissa gives the perigee height and the ordinate axis the magnitude of peak-g values. Corresponding to each value of the prevailing lift-drag ratio $\bar{\varkappa}$ and length L, there is a region in the (h,n) plane.

On each of the curves bounding a region in the(h,n) plane the upper left angular point corresponds to a descent with fixed L/D $\bar{\varkappa}$. This angular point is matched by a fully determined perigee height h_1, which is the lower boundary of the corridor with respect to the height of the perigee. At perigee heights less than h_1, it is impossible to attain the given length by any kind of change-overs making use of the lift for a given L/D.

For perigee heights of $h > h_1$ there is a set of trajectories on which it is possible to attain the necessary length and which provide opportunity for the reduction in g-loading by means of L/D change-over.

On the right, the region is bounded by the upper boundary of the reentry corridor h_3, which corresponds approximately to altitudes of $h_3 \approx 66 - 70$ km, depending on L/D and length. For larger L/D, the limit altitude h_3 is somewhat greater than for lower L/D. Trajectories which have perigee heights

greater than those indicated cannot be projected to the surface of the Earth on the first pass using aerodynamic forces alone.

The graph of Fig.9 contains a region of negative perigee heights. In connection with this, it must be recalled that the perigee height h is a characteristic of the reentry conditions and does not define the altitude of the closest approach to Earth during the initial entry into the dense layers of the atmosphere. This altitude, for most of the trajectories, is not less than 50 km.

The upper boundaries of the regions in Fig.9 correspond to descent trajectories with a single change-over of L/D from negative to positive. Each point on the curve defines the peak-g on the descent trajectory, characterized by the perigee value equal to the abscissa index for that point. There exists a single-valued relationship between the perigee height and the instant of change-over at which the trajectory has the given length. It is clear from the graph that the introduction of a one-time change-over of L/D from negative to positive leads to a notable reduction in g-loading only for perigee heights close to h_3.

The g-loading at the upper boundary of the region represents the largest limit values of g-loading during a descent with two L/D change-overs when the instant of the initial change-over $t_1 \rightarrow t_0$, and the pattern with two change-overs degenerates into a pattern with a single change-over. The points in a region situated below its upper boundary correspond to a descent having two change-overs with a perigee height equal to the abscissa index for that point.

The upper boundary of the region in Fig.9 depends on the length of the   <u>/14</u> descent path. With an increase in length of the descent path, the g-loading is reduced and the upper boundary of the region is shifted downward. In addition,

13

the angular point corresponding to a descent with a fixed L/D is displaced
along the lower left boundary of the region common to the family of regions for
one and the same prevailing L/D but for different lengths of the descent path.

Of greatest interest is the lower boundary of the region since it is there
that the lowest g-loading values occur. The lower boundary of the region can
be divided into two segments which correspond to the two portions of the re-
entry corridor. The first segment, which corresponds to the first portion of
the reentry corridor, begins at the angular point and is practically rectili-
near. In the second portion of the reentry corridor, the lower boundary devi-
ates noticeably from a straight line.

In the first portion of the reentry corridor, the initial g-load maximum
is largest and represents the determining factor; the succeeding maxima do not
exceed the first. For trajectories coming in the first portion, the instant of
the initial L/D change-over is found to occur after passage of the first g-
loading maximum, i.e., at positive L/D. It follows from this that the g-loading
in the first maximum, in the case under consideration, must coincide with the
g-loading in the first maximum for trajectories of a descent with a fixed L/D
equal to the value of the prevailing L/D $\bar{\varkappa}$. This means that the first segment
of the lower boundary in Fig.9 should coincide with the thin line in Fig.2
(i.e., the line which changes into a dot-dash line), corresponding to the same
value of $\bar{\varkappa}$.

On the first portion of the reentry corridor, no maneuver is possible by /15
means of subsequent change-overs for reducing the magnitude of the first maxi-
mum, which is the determining one. Therefore, on this portion, from the point
of view of minimizing the peak-g, it is useless to apply a pattern with more
than two change-overs.

The lower boundary on the first portion depends only on the prevailing L/D. On the second portion, the lower boundary may depend both on the length of the descent path and on the pattern of change-overs. The graph in Fig.9 shows that an increase in the length of the descent path and an increase in the number of change-overs may lead to a reduction in the peak-g on the second portion. However, there are certain limit values below which peak-g cannot be reduced. These limit values correspond to g-loads at the last maximum and, numerically, are close to the g-loads during reentry from decaying satellite orbits (Bibl.2), approximately equal to n = 2 for $\bar{\varkappa}$ = 0.5; n = 2.5 for $\bar{\varkappa}$ = 0.3; and n = 3 for $\bar{\varkappa}$ = 0.2.

As indicated by the graphs in Fig.9, for a prevailing L/D of $\bar{\varkappa}$ = 0.2 and $\bar{\varkappa}$ = 0.3 the lower boundary on the second portion occupies the lower limit position for both the 5000-km and 10,000-km lengths of the descent path.

The entire lower boundary is common to the family of regions which depends on the prevailing L/D. Attainment of the lower boundary is ensured by using a pattern with two change-overs.

As follows from Fig.9, for an L/D of $\bar{\varkappa}$ = 0.5 the lower boundary depends <u>/16</u> on both the length of the descent path and the pattern of change-over. For a length L = 10,000 km, as calculations have demonstrated, the lower boundary already occupies the limit position in the case of a pattern with two change-overs. For a length L = 5000 km, the lower boundary of the region on the second portion, in the case of a pattern with two change-overs, is situated higher than the limit position. An increase up to four in the number of change-overs, as can be seen from the graph, enables the lower boundary to approach the limit position.

BIBLIOGRAPHY

1. - Standard Atmosphere, Gov. Stand. 4401-64 (Standartnaya atmosfera GOST
   4401-64). Izdatel'stvo Standartov, Moscow, 1964.

2. Chapman: Approximation Method for Investigating Entry into Planetary
   Atmospheres (Priblizhennyy metod issledovaniya bkhoda tel v atmosfery
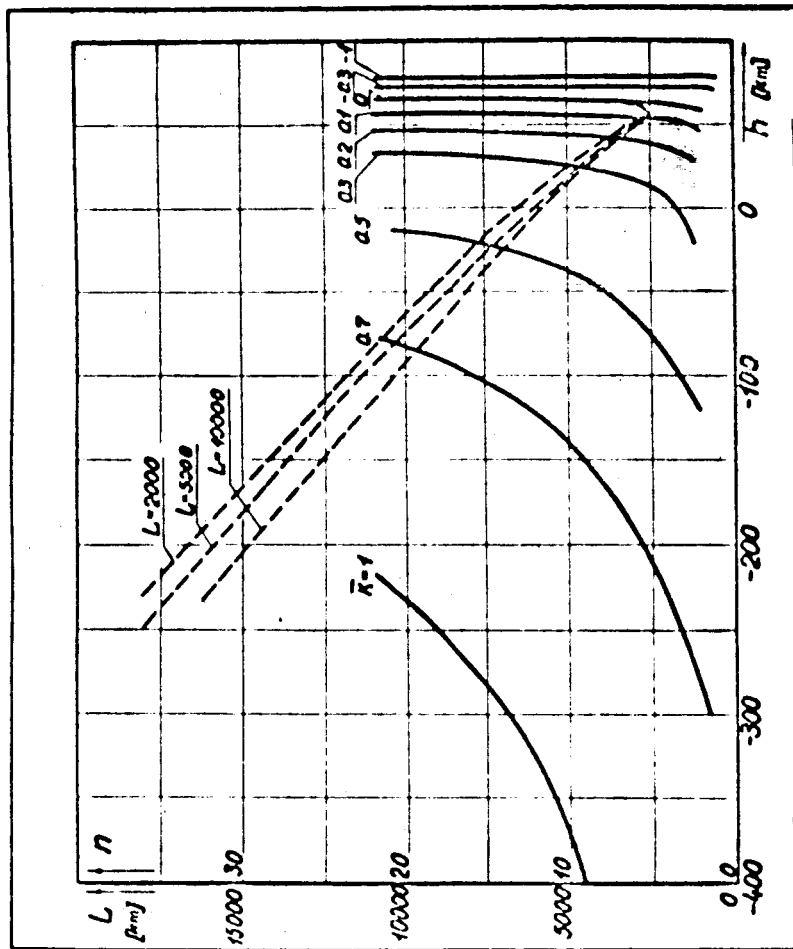   planet). Izd. Inostran. Literatury, Moscow, 1962.

Fig.1 Length of Descent Path L and G–Loading n as a Function of
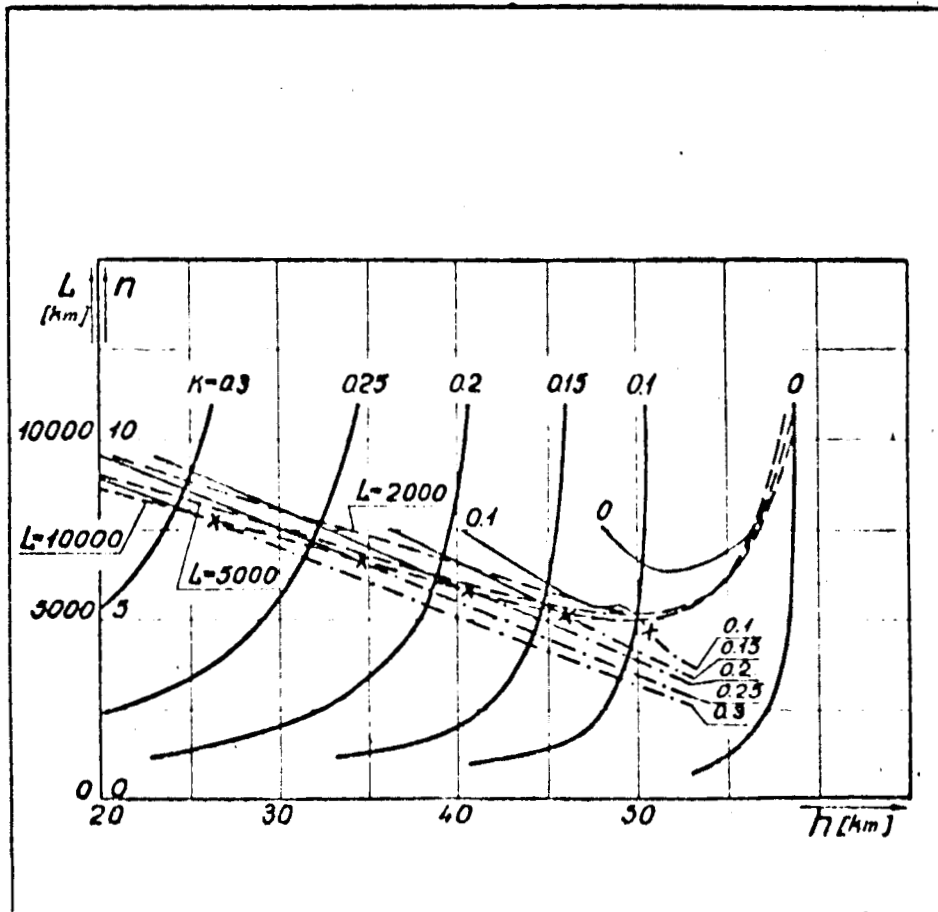Perigee Height on a Descent with Fixed L/D

———— Length
– – – – G–loading at a given length

17

Fig.2 Length of Descent Path L and G—Loading n as a Function of
       Perigee Height on a Descent with Fixed L/D ($\varkappa \leq 0.3$)

         — — — —   G—loading for a given length
         —— ·—·—   G—loading for a given L/D
         ————————   Length
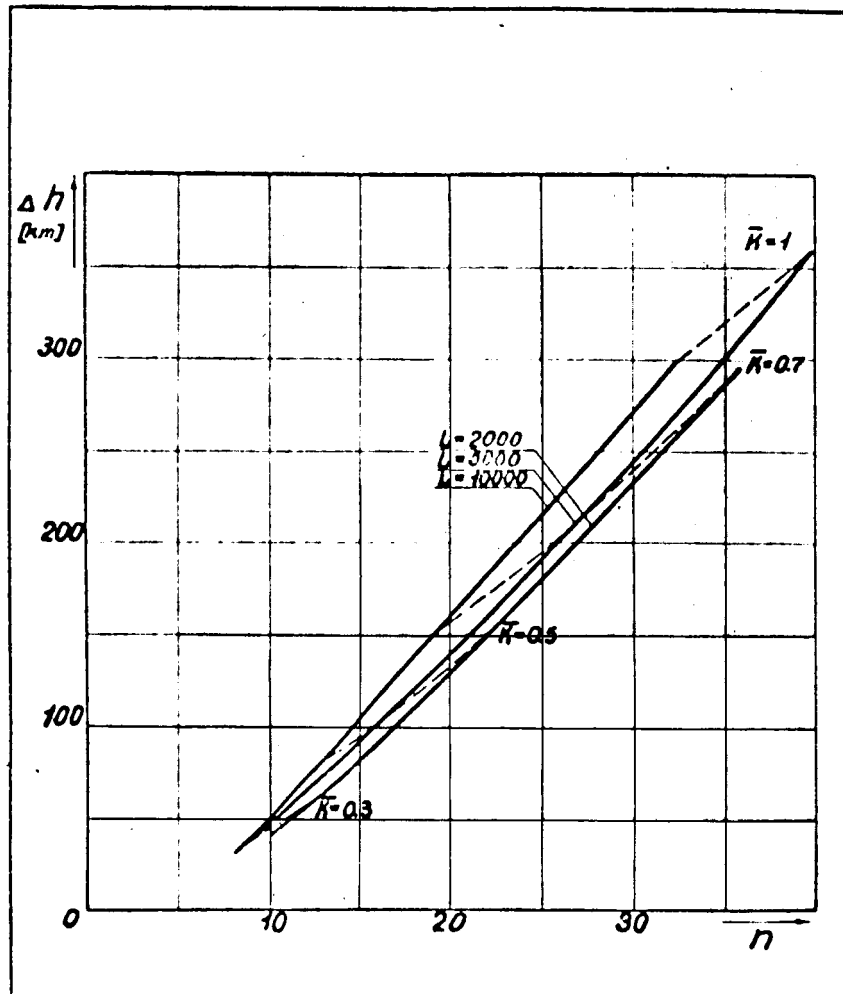
Fig.3 Width of Reentry Corridor   Δh as a Function
              of Allowable G-Loading n

—————— Lines L = const
– – – – Lines $\overline{\varkappa}$ = const
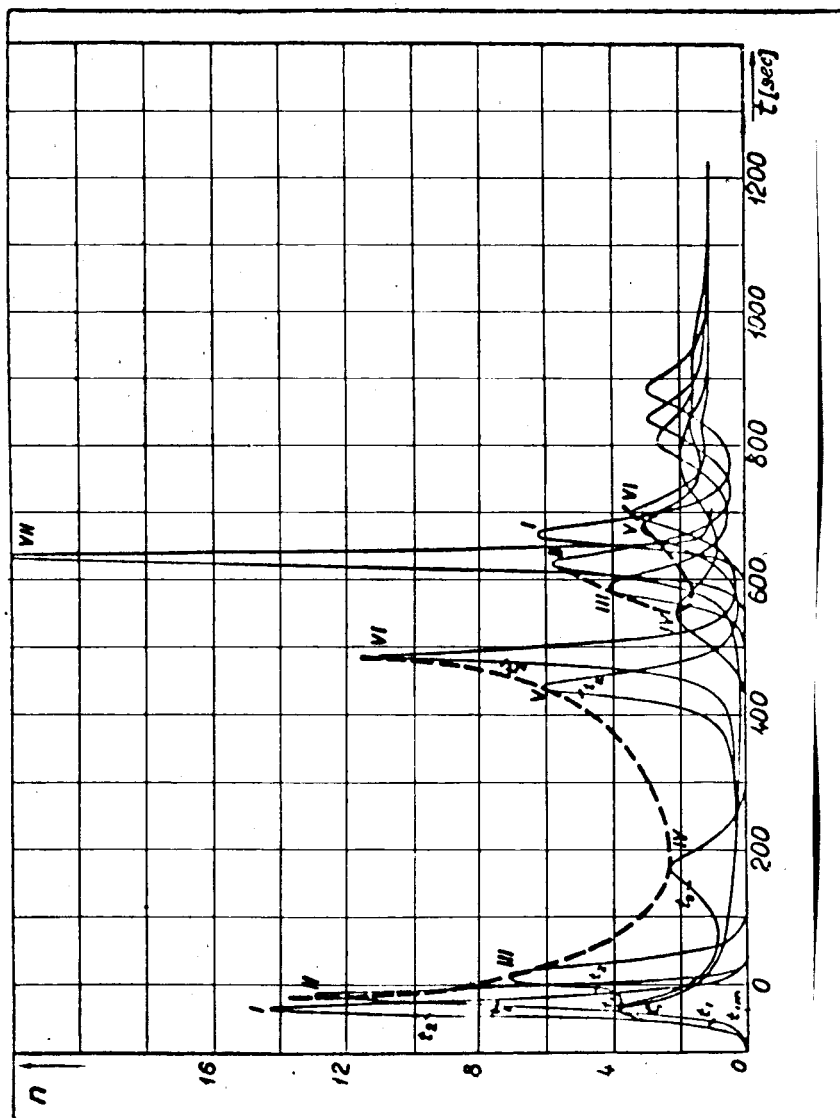
Fig.4 Altitude and G-Loading as a Function of Time

——— Rounded curve of g-loading maxima

h = 44 km, ϰ = 0.5, L = 5000 km
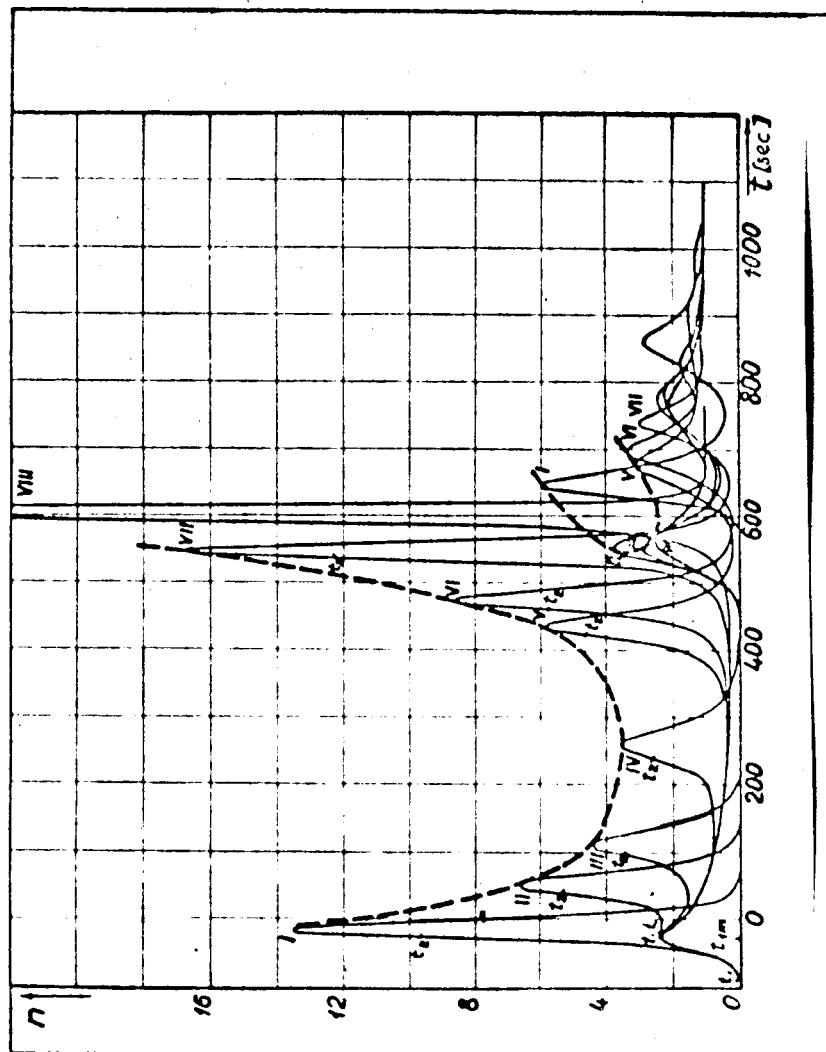
Fig.5   Value of G-Loading as a Function of Time for
Different Values of t_1
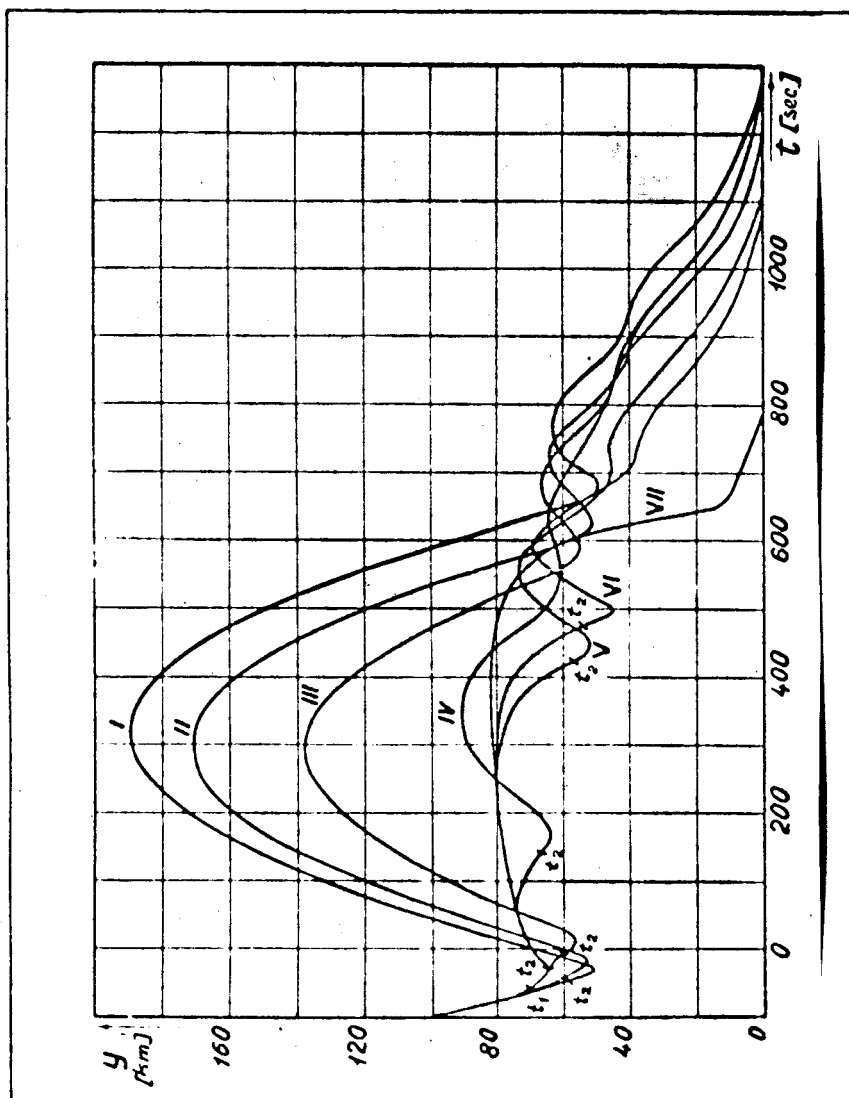
$h = 54$ km, $\varkappa = 0.5$, $L = 5000$ km

Fig.6 Altitude as a Function of Time for Different Values of t_1
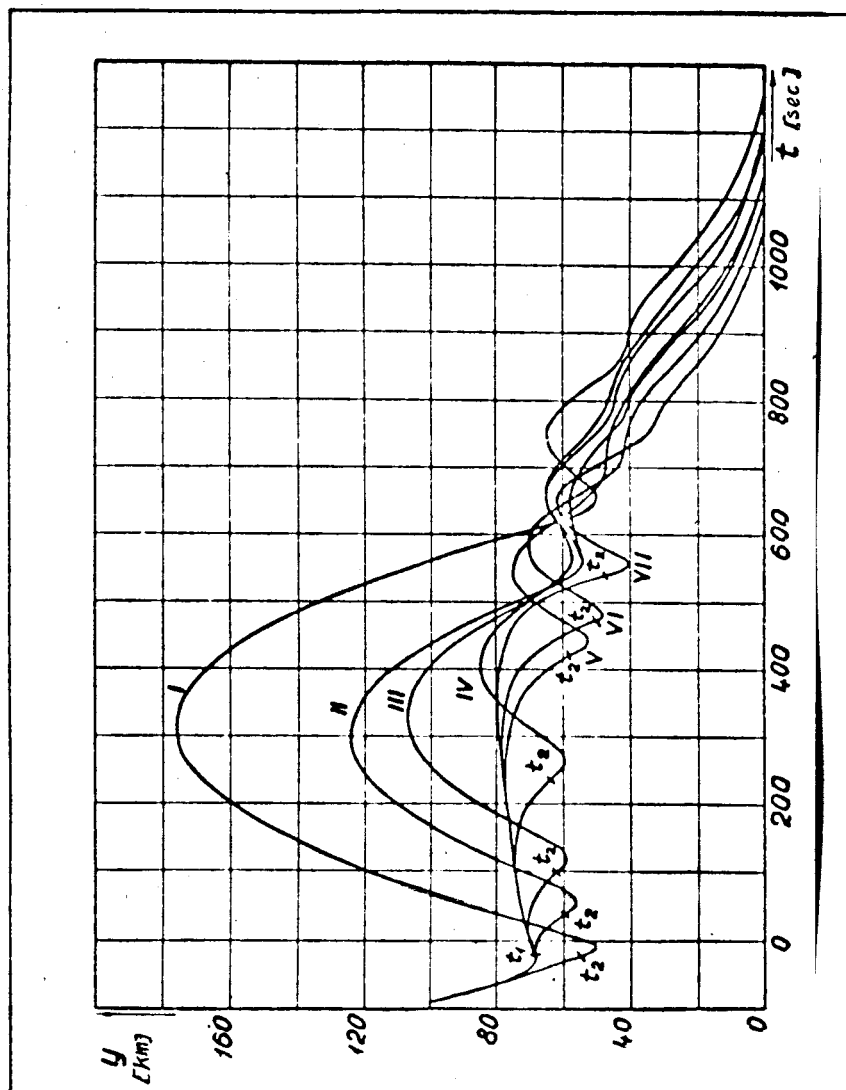
$h = 44$ km, $\varkappa = 0.5$, $L = 5000$ km

Fig.7 Altitude as a Function of Time for Different
Values of t_1

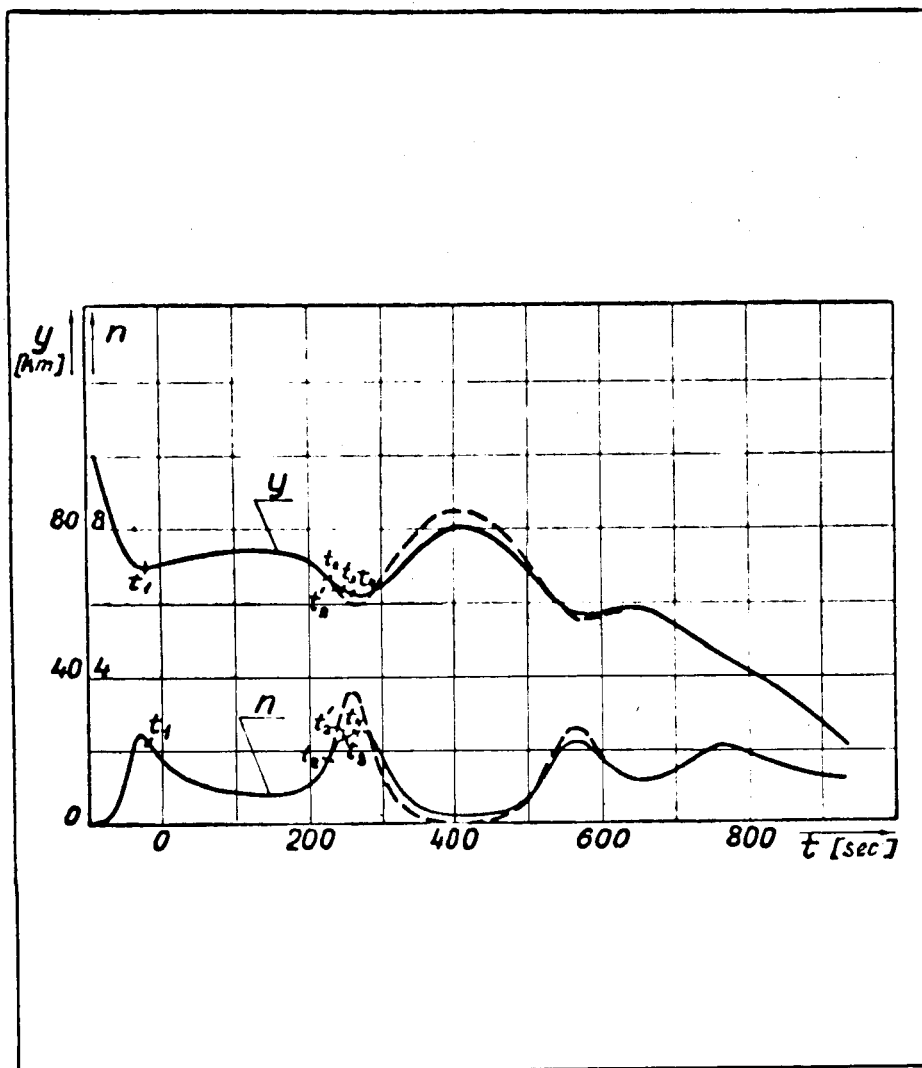$h = 54$ km, $\varkappa = 0.5$, $L = 5000$ km

Fig.8   Value of G—Loading n and Altitude y as a Function
        of Time for Trajectories with L = 5000 km,
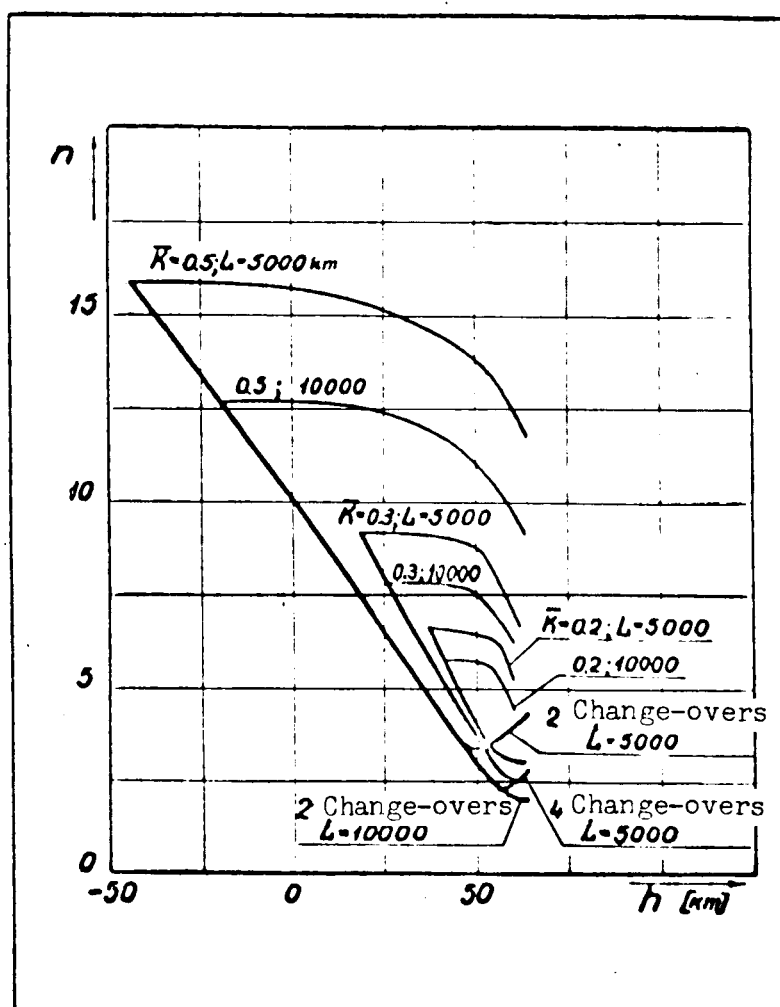   κ = 0.5, h = 54 km

        Four change-overs
        Two change-overs

Fig.9 Boundary of the Region of Possible G—Loads